Experimental Demonstration of Acceleration and Focusing of Magnetically Confined Plasma Rings

James H. Hammer, Charles W. Hartman, and James L. Eddleman
Lawrence Livermore National Laboratory, Livermore, California, 94550

Harry S. McLean
Department of Nuclear Engineering, University of California, Berkeley, California, 94720
(Received 27 June 1988)

We have demonstrated acceleration of magnetically confined plasma rings in a coaxial accelerator, with acceleration of 0.02-mg ring masses to 1.4×10^{8} cm/sec at $\gtrsim 30\%$ efficiency. In some cases low-mass rings have reached a velocity of 2.5×10^{8} cm/sec. When the accelerated rings translate into conical electrodes, we have observed focusing of rings by a factor of ~ 3 in radius, with a factor of $\gtrsim 4$ magnetic field amplification. A reasonably complete accounting of ring mass, momentum, and energy confirms the basic concept of acceleration of stable, well-confined magnetized plasma rings.

PACS numbers: 52.55.Hc, 52.75.Di

In this Letter we describe results of the ring acceleration experiment (RACE), which was initiated to prove the principle of a new type of collective accelerator based on magnetically confined plasma rings.[1] The motivation for developing this technology is to reach high power and high-energy density with accelerated and focused rings for a wide range of applications. These include an intense x-ray source that at very high powers could serve as an efficient driver for inertial-confinement fusion.[2] At less demanding conditions than required for inertial-confinement fusion, the plasma ring accelerator can be applied to fueling and current drive in magnetic fusion devices, generation of ultrahigh-power microwaves, and as a power-amplifying fast opening switch for pulse power applications.[3]

Magnetic confinement of plasma in the rings is the key feature of the accelerator concept. This distinguishes the concept from earlier devices that employed magnetic acceleration of unconfined plasma.[4,5] The plasma is confined by a nearly force-free, compact torus field structure consisting of a dipolelike poloidal field with an entrapped toroidal field as shown in Fig. 1, produced by currents flowing in the plasma and image currents in nearby conductors. The ring field and confined plasma is magnetically accelerated in the coaxial electrode configuration shown in Fig. 1 with the ring acting as a moving armature as in a coaxial rail gun. Shear of the ring field provides a stability threshold against the Rayleigh-Taylor instability[6] as the ring is accelerated. The theoretical stability limit found from ideal MHD ballooning mode calculations[7] is $\kappa < 0.4$, where κ is the ratio of the accelerating force to the ring magnetic force, $\kappa = B_{\rm acc}^2/B_{\rm ring}^2$. Experimentally, we have subjected the rings to accelerating forces such that $\kappa \lesssim 1$ without evidence of gross disruption.

Stability of the confined plasma and field configuration, and long confinement times allow us to accelerate the ring over large distances compared to the characteristic ring dimensions and to a directed kinetic energy much greater than the internal magnetic and thermal energy of the ring. A directed kinetic energy ≈ 10 times the internal magnetic energy of the compact torus has been reached in RACE. The internal magnetic energy of the ring is typically much greater than the thermal energy.

When a high ratio of kinetic to magnetic energy has been achieved, focusing to high energy and power density is achieved by the translation of the rings into conical electrodes. The ring momentum carries the ring toward the apex of the cone, compressing the compact torus fields which are constrained to lie between the electrodes and focusing the confined plasma. Compression of ring magnetic fields increases the ring magnetic energy at the expense of kinetic energy, and leads to reflection of the ring if the compression ratio is too large. Additionally, the focusing time scale must be sufficiently long to allow the ring to undergo self-similar compression and to avoid exciting shock waves that impede focusing. Most applications of focused rings employ a compression ratio less

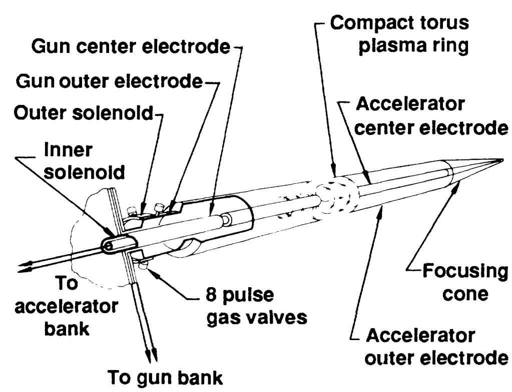

FIG. 1. The ring acceleration experiment apparatus, consisting of a magnetized plasma gun, a set of linear coaxial acceleration electrodes, a focusing cone at the end of the accelerator, and a vacuum system.

than that which would cause reflection, so the bulk of the energy at the deposition point remains directed kinetic energy. Focusing in conical electrodes could allow a compact torus accelerator scaled to several tens of megajoules to reach power densities required for x-ray generation ($\gtrsim 10^{13}$ W/cm^2) and ultimately for inertial fusion ($\gtrsim 10^{15}$ W/cm^2).

The plasma rings are produced by a magnetized coaxial plasma gun at the beginning of the accelerator shown in Fig. 1. The gun is 50 cm long with an outer (inner) diameter of 35 cm (20 cm) and has both inner and outer solenoids which are energized by a 5-kV, 250-kJ electrolytic capacitor bank. 1–5 atm cm^3 of H_2 gas is then fed into the gun with eight pulse gas valves. The gas is broken down and the plasma and B field are ejected from the gun by the application of a negative voltage to the center electrode from a 60-kV, 200-kJ capacitor bank with an external inductance of $\simeq 50$ nH. As in similar magnetized gun experiments,[8–10] firing the gun results in emergence of a spheromak-type compact torus near the gun muzzle. In RACE, the ring is formed in the interelectrode region at the beginning of the accelerator section (see Fig. 1). The straight coaxial accelerator electrodes were initially 6 m long with an outer (inner) diameter of 50 cm (20 cm), and are housed in a vacuum vessel 1.5 m in diameter. Conically converging electrodes for ring focusing have been substituted for the final 2 m of straight electrodes during the most recent operations as shown in Fig. 1. Rings are accelerated axially by $\mathbf{J}\times\mathbf{B}$ forces when the 260-kJ, 120-kV accelerator bank is discharged. The accelerating B_θ field is fed through an annular slot between the inner gun and inner accelerator electrode as shown in Fig. 1.

The diagnostics consist of current and voltage monitors for the banks, visible light and vacuum uv detectors, B-loop probes arrayed circumferentially (for symmetry) and axially (for trajectory), and a helium-neon laser interferometer for the measurement of the line-integrated electron density. Except for early studies examining radial profiles and verifying the compact torus topology of the fields, the B loops have been located near the outer accelerator electrode.

The first experiments with all stainless-steel electrodes demonstrated formation of compact torus rings suitable for acceleration having total magnetic energy of 5–10 kJ and ring lengths of 50–100 cm. Acceleration was observed to $v_{\text{ring}} \approx 4\times 10^7$ cm/sec with a ring mass of 5×10^{-4} g and a kinetic energy of ≈ 40 kJ (out of 100 kJ of accelerator bank energy) inferred from trajectory analysis. The ring mass was not well correlated with the amount of injected gas and was somewhat high for matching the transit time of the ring to the quarter cycle time of the accelerator bank, or equivalently matching the impedance of the bank to the accelerator. Subsequent experiments have been conducted with tantalum liners on the gun and accelerator electrodes, and glow discharge cleaning. Electrode contributions to the ring mass have been reduced, resulting in acceleration up to $v \approx 2.5\times 10^8$ cm/sec. Formation of lower-mass rings is a sensitive function of gun parameters, particularly of gas inlet timing. If the gas inlet is timed such that the gas just reaches the opposing gun center electrode when the gun is fired, a distinct low-mass ring can be formed with little trailing effluent. When the gas is allowed too long a time to extend into the gun region, a protracted "tail" that can interfere with acceleration is observed with the magnetic probes.

Our proving the principle of ring acceleration has required demonstration of several significant features. The most fundamental of these is the observation of the integrity of the ring under acceleration. Figure 2 shows the time dependence of the axial magnetic field (B_z) observed by a probe at the outer electrode as a ring moves down the accelerator. The ring B_z field at the electrode is typically 3–10 times the ring B_θ field (an ideal spheromak-type ring has $\mathbf{B}=B_z\hat{\mathbf{z}}$ only at the outer electrode). The accelerating B_θ field is observed to rise sharply behind the ring. Assuming a nearly constant velocity of the ring as it passes the magnetic probe allows us to identify the time dependence with the axial profile of the magnetic field. We have observed approximate preservation of the ring field profile and intensity for the entire 6 m of the linear acceleration section, with some changes in response to acceleration such as steepening of the trailing edge. Superimposed on the field trace shown in Fig. 2 is the time-dependent line-averaged electron density at the same axial location, indicating that the plasma is well localized to the ring magnetic fields. The line-averaged density provides an estimate of the plasma inventory in the ring and a lower bound on the ring mass found by our assuming a pure hydrogen plasma. For the shot shown in Fig. 2, the bound on the ring mass is 8 ± 1.5 μg with the uncertainty set by the estimate of ring velocity and the radial density profile.

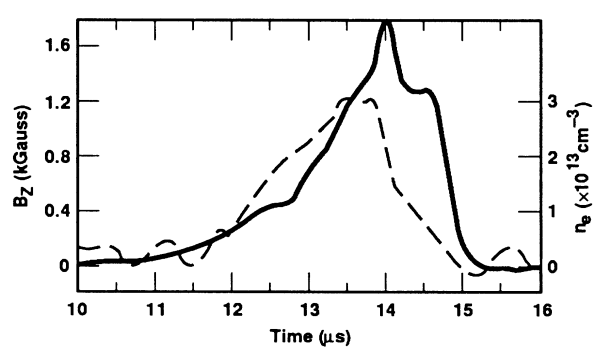

FIG. 2. The solid curve shows the time-dependent axial magnetic field measured at the outer electrode, at an axial distance of 1.1 m from the beginning of the accelerator. The radially averaged electron density measured by the interferometer at the same axial location is shown by the dashed curve.

Other important features for our proving the concept are the consistency of momentum and energy balance. Given the ring mass and the applied force on the ring derived from the electrical circuit properties, we can calculate the trajectory and compare it to the trajectory observed with probes. For this purpose we use a point model of ring acceleration which treats the ring as a localized, constant mass with zero resistance. The ring is assumed to obey a force equation where ring inertia is balanced by the magnetic accelerating force and the resistive drag of the metal electrodes. A circuit equation is simultaneously solved with a time varying inductance determined by the ring position:

$$\ddot{L}_t I + I/C = 0\,, \tag{1}$$

$$L_t = L_x + L'l\,, \tag{2}$$

$$M\ddot{l} = F_{\mathrm{TOT}} = \tfrac{1}{2}L'I^2 - F_{\mathrm{DRAG}}\,, \tag{3}$$

where I is the current, L_t is the total inductance, L_x is the external inductance, L' is the inductance per unit length of the accelerator, C is the accelerator bank capacitance, M is the ring mass, and l is the ring axial position.

The dashed curve in Fig. 3 shows the point-model calculation for the ring trajectory for the shot shown in Fig. 2 with the estimated ring mass of 8 μg. Figure 3 also shows the ring trajectory measured by magnetic probes with horizontal bars to indicate the full width at half maximum of the axial magnetic field measured at each probe location. The consistency of the trajectory calculated by momentum balance with the observed trajectory indicates that the actual ring mass is within about 30% of the lower bound mass determined by the interferometer. The trajectory can be determined by a third and independent method using the accelerator bank current and voltage data to determine the time-dependent inductance of the accelerator. Neglecting resistance, the accelerator inductance can be found from the measured voltage (V) and current:

$$L_{\mathrm{acc}} = \left[\int V\,dt\right] \Big/ I - L_x\,, \tag{4}$$

and the axial position of the moving short circuit is then,

$$l = L_{\mathrm{acc}}/L'\,, \tag{5}$$

where

$$L' = 2\ln\frac{r_{\mathrm{outer}}}{r_{\mathrm{inner}}}\ \mathrm{nH/cm}\,.$$

The solid curve in Fig. 3 shows the current sheet position as calculated in Eq. (5). The close correlation with the actual trajectory indicates that the current path between electrodes is primarily at the ring. The flattening out of the trajectory late in time is due to the presence of the conical electrodes of the end of the accelerator which cause ring deceleration and reflection. The point-model calculations were terminated before the ring enters the cone.

Energy balance can also be confirmed by our comparing the work done on the moving current sheet, E, given by

$$E = \int^t VI\,dt - \tfrac{1}{2}L(t)I^2 = \int^t VI\,dt - \tfrac{1}{2}I\int^t V\,dt\,, \tag{6}$$

with the ring kinetic energy calculated by the point model, which should be the same in the limit of low ring resistance and drag forces. Figure 4 shows the comparison for the shot shown in Figs. 2 and 3.

Not all shots show the clear evidence of coupling to the accelerator seen in Figs. 2–4. A "restrike" is sometimes observed, particularly when the accelerator voltage is high. The current sheet position determined by Eq. (5) may follow the ring position for a portion of the ac-

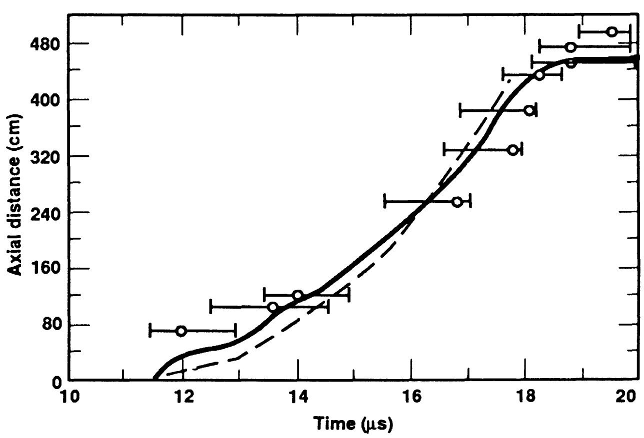

FIG. 3. The ring trajectory (axial displacement vs time) as determined by magnetic probes (horizontal bars), by accelerator voltage and current data (solid curve), and by force-balance calculations (dashed curve).

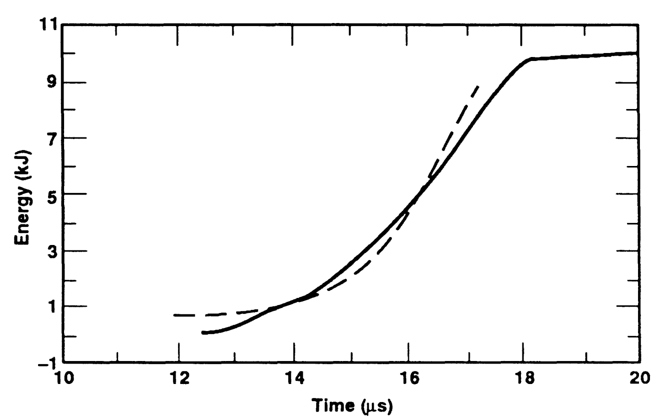

FIG. 4. The ring kinetic energy determined from accelerator current and voltage data (solid curve), and from force-balance calculations (dashed curve).

celerator length and then make a sudden jump back to the vicinity of the accelerator feed slot. The cause of the restrike is not yet understood although it may be related to surface contamination or possibly the "blow-by" effect when the accelerating field exceeds the ring field and blows by the ring, creating large inductive voltage spikes.

We observe ring focusing with an array of magnetic probes distributed along the conical electrode. Several types of behavior are seen as rings impinge on the cone: reflection of the ring completely out of the cone after focusing by factors of 2–3 in radius; partial reflection followed by ring stagnation in the cone; ring stagnation without obvious reflection. The stagnated rings persist for ≈ 100 μsec. The cone converges to a small enough radius so that the rings are generally reflected or stagnated before they can exit from the cone. Field amplification is also observed by factors of order 4, e.g., a 1-kG ring at the entry of the cone compressing to 4 kG at the reflection point of between a factor of 2 and 3 radial compression.

In summary, we have conducted experimental studies of compact torus formation, acceleration, and focusing on the RACE device. The data support the basic concept of a stable, well-confined plasma ring that undergoes acceleration and focusing in a manner consistent with simple models of momentum and energy balance.

We would like to thank T. K. Fowler, John Holzrichter, John Nuckolls, and Bruce Kusse for continued support and useful discussions. We would also like to thank the Department of Energy Office of Basic Energy Sciences under Ryszard Gajewski for their support. This work was performed under the auspices of the U.S. Department of Energy under Contract No. W-7405-Eng-48.

[1]C. W. Hartman and J. H. Hammer, Phys. Rev. Lett. **48**, 929 (1982).

[2]C. W. Hartman, J. L. Eddleman, J. H. Hammer, and D. L. Meeker, in *Proceedings of the Fourth International Conference on Emerging Nuclear Systems, Madrid, Spain, 1986,* edited by G. Velarde and E. Minguez (World Scientific, Singapore, 1987), p. 158.

[3]C. W. Hartman and J. H. Hammer, Lawrence Livermore National Laboratory Report No. LLL-PROP-191, 1984 (unpublished).

[4]J. Marshall, Phys. Fluids **3**, 134 (1960).

[5]D. Y. Cheng, Nucl. Fusion **10**, 305 (1970).

[6]A. B. Mikhailovskii, *Instabilities of an Inhomogeneous Plasma,* Theory of Plasma Instabilities Vol. 2 (Consultants Bureau, New York, 1974), p. 177.

[7]J. H. Hammer, J. L. Eddleman, and C. W. Hartman, Bull. Am. Phys. Soc. **30**, 1449 (1985).

[8]W. C. Turner *et al.*, Phys. Fluids **26**, 1965 (1983).

[9]C. W. Barnes *et al.*, Phys. Fluids **29**, 3415 (1986).

[10]T. Uyama *et al.*, Nucl. Fusion **17**, 799 (1987).